Multi-Element Superconducting Nanowire Single-Photon Detector

Eric A. Dauler, Bryan S. Robinson, Andrew J. Kerman, Joel K. W. Yang, Kristine M. Rosfjord, Vikas Anant, Boris Voronov, Gregory Gol'tsman, and Karl K. Berggren

***Abstract*—A multi-element superconducting nanowire single photon detector (MESNSPD) is presented that consists of multiple independently-biased superconducting nanowire single photon detector (SNSPD) elements that form a continuous active area. A two-element SNSPD has been fabricated and tested, showing no measurable crosstalk between the elements, sub-50-ps relative timing jitter, and four times the maximum counting rate of a single SNSPD with the same active area. The MESNSPD can have a larger active area and higher speed than a single-element SNSPD and the input optics can be designed so that the detector provides spatial, spectral or photon number resolution.**

***Index Terms*—Niobium nitride, photon-counting-array, photon-number-resolution, single-photon-detector.**

I. Introduction

ALTHOUGH photon counters provide the ultimate sensitivity in optical detection, many applications require additional information about the state of the optical radiation, including spatial, spectral and photon-number resolution that most photon counters do not provide. One of two approaches can be taken in order to obtain this information: the optical signal can be spread across a large array of single-photon detectors, so that the information is extracted from the number and position of the detectors that fire, or a photon counting technology can be selected that allows the information to be extracted from a single detector's output signal. The spatial and spectral resolution from a large array can be much better than from a single detector because the resolution of the array is limited only by the number of elements and the optics used to couple the light, not by noise in the detection process or analog readout electronics. Furthermore, an array is more flexible than a single detector, because the same array and readout electronics can be combined with any combination of: (1) imaging optics that provide spatial information, (2) a diffraction grating that provides spectral information, or (3) an optic that spreads the beam across multiple elements to provide photon number resolution and higher counting rates. Finally, the array can be composed of detectors that do not individually resolve information about all of these properties of light, which allows a detector technology to instead be selected to provide high-detection efficiency, low dark count rate, or excellent timing resolution.

However, there are also disadvantages to using arrays of photon counting detectors. First, there is typically an optical coupling loss associated with a microlens array or non-unity fill factor. Second, some photon counters require a significant amount of discrete electronics or cannot be fabricated on a single wafer, so arrays may be expensive or bulky. Third, many problems faced by single detectors, such as fabrication yield and dark counts, are multiplied when arrays of photon counters are needed. Finally, there are additional challenges that arise in arrays, such as crosstalk between elements and providing readout for each detector in a large array.

The MESNSPD approach proposed here alleviates many of these disadvantages, particularly when the input optics are configured so that the MESNSPD provides photon number resolution and higher counting rates. The first disadvantage of photon counting arrays discussed above, the additional optical loss associated with coupling light into the array versus a single detector, is eliminated by the MESNSPD design. The MESNSPD differs from conventional arrays of photon counters because there are no gaps between elements: the elements are lithographically patterned such that the combined active area is indistinguishable optically from that of a single-element detector. This uniformity eliminates the coupling loss associated with a microlens array or non-unity fill factor. Second, a packaged MESNSPD is unlikely to be large or expensive because hundreds of SNSPDs can be fabricated on a single chip [2] and the electronics required to operate a SNSPD are simple because SNSPDs do not require an external reset circuit. Third, although fabrication yield and the scaling of dark counts will need to be addressed, the MESNSPD design provides a unique opportunity to alleviate these challenges. If the optical beam is to be spread across multiple elements to provide higher counting rates or photon-number resolution, the MESNSPD elements can be fabricated with active areas smaller than a focused optical spot. Using smaller, contiguous elements that are illuminated by a single, tightly focused beam provides several advantages compared to larger, isolated elements: smaller SNSPDs can have faster reset times, because this time is limited primarily by the kinetic inductance of the nanowire [3], and smaller elements are also likely to have lower dark count rates and higher fabrication yields.

Manuscript received August 25, 2006. This work was supported by the US Air Force under Contract FA8721-05-C-0002. Opinions, interpretations, recommendations, and conclusions are those of the authors and are not necessarily endorsed by the US government.

E. A. Dauler is with the Massachusetts Institute of Technology, Cambridge, MA 02139 USA and also with the Lincoln Laboratory, Massachusetts Institute of Technology, Lexington, MA 02420 USA (e-mail: edauler@mit.edu).

B. S. Robinson and A. J. Kerman are with the Lincoln Laboratory, Massachusetts Institute of Technology, Lexington, MA 02420 USA.

J. K. W. Yang, K. M. Rosfjord, V. Anant, and K. K. Berggren are with the Massachusetts Institute of Technology, Cambridge, MA 02139 USA.

B. Voronov and G. Gol'tsman are with Moscow State Pedagogical University, Moscow, Russia.

Color versions of one or more of the figures in this paper are available online at http://ieeexplore.ieee.org.

Digital Object Identifier 10.1109/TASC.2007.897372

The final drawbacks to photon counting arrays mentioned above are the challenges associated with scaling to large array sizes and the potential for interactions between array elements; these drawbacks and the advantages of the MESNSPD design are addressed in the remainder of this paper. Some of the challenges associated with scaling the MESNSPD approach to large array sizes are discussed briefly in the next section, in which the design and fabrication of a two-element MESNSPD is also presented. A series of experiments to study the interactions between the elements of a two-element SNSPD are discussed in the third section. Measurements of the noise count rate, the detection efficiency and the timing jitter showed no interaction between the two detector elements due to detection events in the adjacent element. Finally, the performance improvements provided by the MESNSPD approach are demonstrated. It is shown that even a two-element SNSPD can be useful if light is spread evenly across both elements: the two-element SNSPD can simultaneously resolve more than one photon and also has roughly four times the maximum counting rate of a single SNSPD with the same active area. This configuration is useful for Hanbury-Brown Twiss [4], [5] measurements and applications requiring very high counting rates, such as optical communications [6]. Although the two-element SNSPD used in this work was biased and read out using discrete electronics, future efforts to integrate these functions on chip could make this approach useful for arrays with more elements designed for applications such as spectroscopy [7], laser radar [8] and quantum optics [9].

II. MESNSPD Design and Fabrication

Superconducting nanowire single photon detectors (SNSPDs; also referred to as SSPDs [1]) are composed of a thin, narrow superconducting wire that is biased slightly below its critical current. The absorption of a photon in the wire depletes the number of superconducting carriers in a small region, reducing the critical current density such that the critical current is exceeded and a small length of wire becomes resistive [10], [11]. In order for this resistive region to form as a result of the absorption of single infrared photons, the wire dimensions must be small: approximately 4 nm thick and 100 nm wide NbN wires are used both in this work and previous work [2]. It has been shown previously [2] that the detection efficiency of SNSPDs with these dimensions can be as high as 57% at 1.55 μm wavelength after the addition of an optical cavity and anti-reflection coating, although neither were added to the devices presented in this paper. In order to increase the active area over which a photon can be absorbed, the wire is typically written as a boustrophedonic pattern (a meander with straight segments), as shown for a typical SNSPD in Fig. (1a). The gaps between wires are also typically 100 nm, highly sub-wavelength for IR photons, resulting in an absorption that can be described by an effective index of refraction [12], but does not limit the detection efficiency to the ratio of area covered by wire [2]. The active area, which is composed of straight segments of wire that are connected (shorted) on alternate ends, is thus a continuous optical element at the IR wavelengths of interest. The identical active area exists if an extra lead is added from one of the connections between nanowire segments, allowing the active area to be split into two separate wires (Fig. 1b). Similarly, more leads can be added in this fashion in order to split the active area into more elements. The maximum number of elements in a MESNSPD is limited by the need to connect contact pads to each element. The devices were fabricated using a scanning-electron beam lithography process described previously [13] including the modifications to the process for fabricating bare devices (without cavity or anti-reflection coating) described in reference [2].

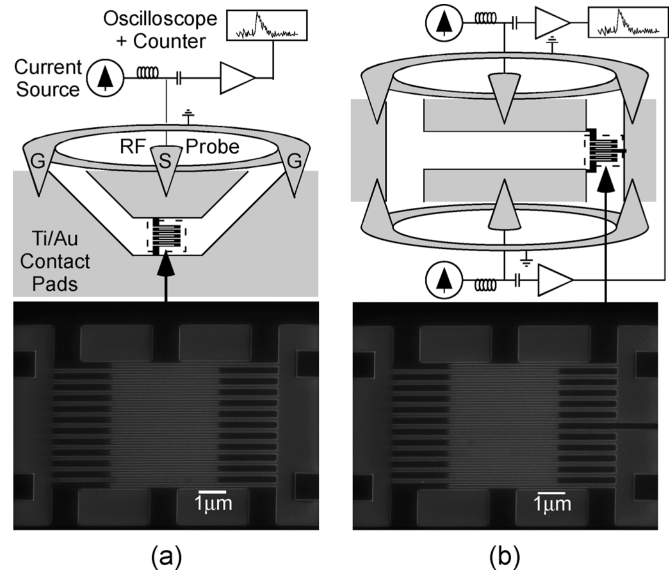

Fig. 1. (a) Schematic of the test setup and scanning-electron-microscope (SEM) micrograph of a single SNSPD; (b) schematic of the test setup and SEM micrograph of a two-element SNSPD with the identical active area as the SNSPD shown in (a).

III. MESNSPD Testing and Performance

A. Crosstalk and Interaction Between Array Elements

Ideally, the multiple detector elements composing a MESNSPD would not interact, so that the electrical output from each element would accurately reflect its optical input. In practice, various types of interactions between the elements can limit the utility of an array. Crosstalk might be expected due to coupling of electromagnetic fields or the generation of phonons during a detection event, so it is important to test whether one detector element firing affects adjacent elements.

Several tests were performed on the two-element SNSPD in order to verify that each element was behaving independently. These tests were performed using the same cryogenic probing station setup described in [2] and [3], with the addition of a second readout channel that included an RF electrical probe, bias T, battery-powered current source, attenuator, amplifier and DC block (Fig. 1b). The detector was optically illuminated through the sapphire substrate using a focused spot from a fiber-coupled lens assembly, which was also mounted on a micromanipulated arm. The electrical output from each detector element was connected to a 6 GHz real-time oscilloscope or a pulse counter.

The first test performed to characterize the two-element SNSPD was a measurement of the critical current of each detector element. The bias currents in both detector elements were adjusted and the critical current for a given element did not change measurably as the current in the adjacent element was adjusted over the range in which it remained superconducting. When the critical current was exceeded and heat was continually dissipated in one of the nanowires, the critical current of the adjacent nanowire decreased by more than 10%, which we believe was due to local heating. The measurements discussed in the remainder of this paper were made with both elements in the superconducting state, biased at approximately 95% of their respective critical currents, except where otherwise noted.

Next, the timing jitter of the MESNSPD was measured to determine if interaction between elements might be detrimental to the device timing. An optical input was provided consisting of < 1 ps, 1550-nm-wavelength optical pulses generated at a 10 MHz repetition frequency from a passively mode-locked fiber laser. The intensity of these pulses was adjusted such that the probability of obtaining a detection event was roughly 10% for each detector element per optical pulse. An optical splitter was used to direct a portion of the light to a 40 GHz photodiode whose output was also connected to the oscilloscope. The front edge of one detector element's output signal was used to trigger the oscilloscope and the timing of the front edge of the photodiode output was measured. This allowed the timing jitter of each element's output to be measured, as the timing jitter of the photodiode output was negligibly small. The obtained histograms (Figs. (2a) and (2b)) show that the two detector elements each have a timing jitter of 29 ps FWHM. Next, the relative timing jitter of the two detector elements was measured. For this measurement, the oscilloscope continued to be triggered by the front edge of one detector element's output while the timing jitter of the front edge of the second element's output signal was measured. The histogram of this relative timing jitter is shown in Fig. (2c). This timing jitter closely matches the prediction based on the convolution of the timing jitter measured for each element independently, confirming that the jitter in each detector element is independent. We believe this measured 44 ps FWHM coincident timing jitter is the best reported for a pair of single photon counting detectors, making the MESNSPD an attractive candidate for Hanbury-Brown Twiss measurements [4], [5].

The two-element SNSPD was also tested for crosstalk, where a noise count occurs in one element due to a detection event in the adjacent element. In this case, the laser input to the device was blocked and the electrical arrangement was identical to that used to measure the relative timing jitter. The detector elements were illuminated with low-intensity background light that had constant intensity and can be well approximated by Poisson statistics. The background light counts from one detector element were used to trigger the oscilloscope and the number of coincident noise counts from the second element was measured. The intensity of the background light was adjusted such that the count rate in the second detector was 100 kHz. An output pulse was considered coincident whenever it occurred within a 1 ns time period, centered on the timing of coincident events as determined from the relative timing jitter measurement. After 750,000 detection events in the element used to trigger the measurement, 80 coincident detection events were observed in the adjacent detector element. If the counts in the second detector were uncorrelated to those in the triggering detector, 75 coincident detection events would be expected within 750,000 1 ns time windows. Therefore, the measured crosstalk, 0.0007% ($\pm$0.001%), is within the noise of the measurement.

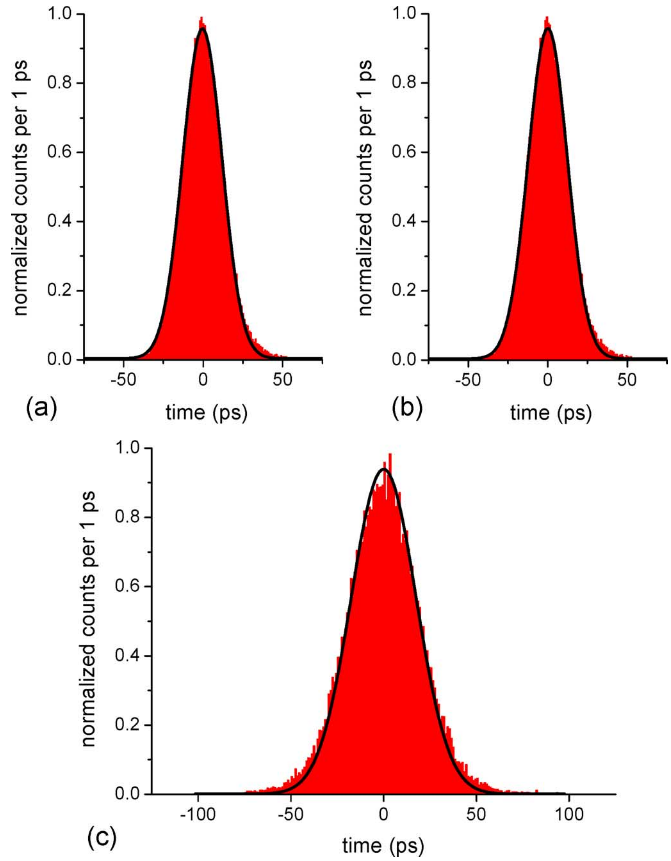

Fig. 2. (a) and (b) Histogram of the timing jitter of each detector element measured relative to the illuminating optical pulse and a Gaussian fit (line) showing 29 ps FWHM timing jitter; (c) histogram of the timing jitter of one detector measured relative to the adjacent detector and a Gaussian (line) calculated by convolving the fits from (a) and (b), demonstrating that the timing jitter from each element is uncorrelated during a two-photon detection event.

Finally, the detection efficiency of the devices was measured to look for any evidence of an interaction between the device elements. The optical and electrical setup used to measure the detection efficiency was the same as that used to measure the timing jitter except for the way the oscilloscope was triggered. First, only one of the detector elements was biased at various critical currents while the other element was left unbiased. The oscilloscope was triggered using the photodiode output and the detector element's output was connected to another oscilloscope channel. The detection efficiency was measured by comparing the number of detection pulses in a 1 ns time period, centered to capture detection events from the optical pulses, to the total number of trigger events. Second, the adjacent detector element was biased at 95% of its critical current and the oscilloscope was triggered by its output. The detection efficiency of the first detector element was measured by comparing the number of detection pulses in a 1 ns time period to the number of trigger events, which in this case restricted the measurement to only those optical pulses from which a photon was detected by the adjacent

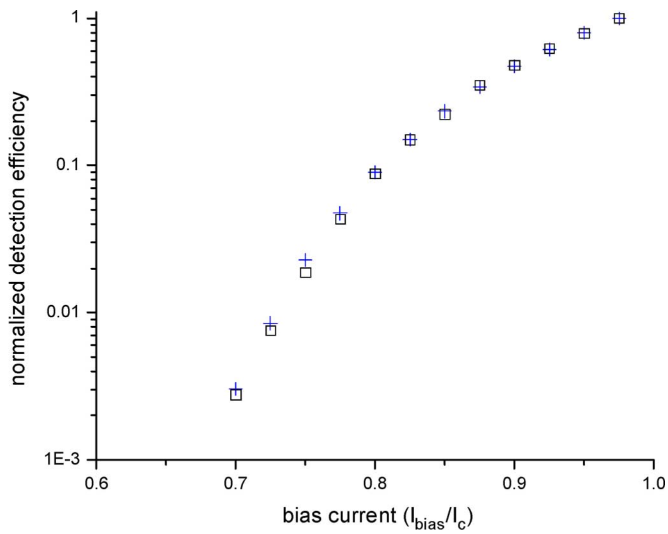

Fig. 3. Normalized detection efficiency of a single detector element measured with the adjacent element unbiased (open squares) and conditioned on the adjacent element firing (blue crosses). A single factor, one over the detection efficiency at $I_{bias}/I_c = 0.975$ with the adjacent element unbiased, was used to normalize both data sets.

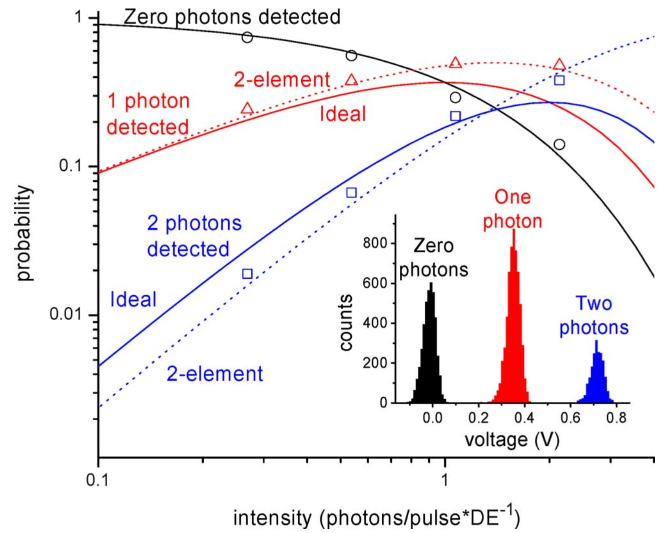

Fig. 4. Theoretical probability of detecting zero, one, or two photons as a function of optical intensity using a two-element single-photon detector (dashed lines) and an ideal photon-number-resolving detector (solid lines). The two-element detection probabilities vary by $\leq$ 3 dB from the ideal detection probabilities for intensities $<$ 2.5 photons. The measured probabilities of detecting zero (black circles), one (red triangles), or two (blue squares) photons are also shown. The inset shows the excellent SNR of the summed analog output signal for distinguishing zero, one, and two detected photons.

element. Thus, the detection efficiency without the adjacent detector element biased can be compared to the detection efficiency conditioned on the adjacent element firing. Fig. 3 shows both of these measured detection efficiencies. There was no statistically significant difference between the detection efficiency measured with and without the adjacent element biased. Therefore, the measurements of the critical current, timing jitter, noise counts and detection efficiency demonstrate that there is no measurable interaction between the adjacent detector elements.

B. *MESNSPD Performance Benefits*

While the MESNSPD provides the opportunity to extract many types of additional information about the input optical photons, as is true for any array of photon counters, this section will instead focus on the performance benefits of a two-element SNSPD. A two-element SNSPD is sufficient to obtain limited photon-number resolution and a higher maximum counting rate by spreading the optical beam evenly across both elements. The fact the MESNSPD provides a continuous optical active area, without gaps between detector elements, permits the optical elements to be smaller than the focused optical spot. In this configuration, a two-element SNSPD can simultaneously resolve two photons. The speed of the MESNSPD is increased in two ways relative to a single SNSPD with the same active area: by a factor of two due to the lower kinetic inductance of each element [3] and by a second factor of two due to the fact there are multiple elements, each counting simultaneously.

First, in order to investigate the two-element SNSPD's ability to resolve multiple photons, we may measure the probability that zero, one, or two elements fire as a function of optical intensity. The optical and electrical setup used to measure these probabilities was the same as that used to measure the timing jitter and detection efficiency, except that the photodiode output was used to trigger the oscilloscope and the number of detection events was extracted by adding the output traces from each detector element after analog-to-digital conversion. Although it is preferable to threshold each output signal separately and digitally add the number of detected photons when a large number of elements are used, the signal to noise ratio of the summed output trace was sufficient to clearly distinguish zero, one and two detection events from the summed analog trace (Fig. 4 inset). The measured probability of detecting zero, one, or two detected photons as a function of optical intensity is shown in Fig. 4.

Additionally, two sets of theoretical curves are also shown in Fig 4: dashed curves showing the expected probabilities for a two element array and solid curves showing the expected probabilities for an ideal photon-number-resolving detector with the same detection efficiency as the two-element SNSPD. It should be noted that coherent optical radiation was used in both the measurements and theoretical curves, so a non-unity detection efficiency shifts the curves without changing their shape. Although, the detection efficiency plays a crucial role in determining the fidelity with which any photon counter can measure the number of incident photons, Fig. 4 is intended to highlight the penalty associated with using a two-element SNSPD. MESNSPDs with a larger number of elements may be required to reduce this penalty to an acceptable level for some applications, although even the best demonstrated SNSPD detection efficiency [2] will quickly become the dominant limitation to achieving high fidelity. A two-element SNSPD is likely to provide sufficient photon-number-resolving capability to benefit applications such as optical communications [6] and quantum optics [9], but is not sufficient for linear optics quantum computing [14].

In addition to the photon-number-resolution, spreading an optical beam across a two-element SNSPD can provide a higher maximum counting rate. This counting rate can be demonstrated by measuring the probability of detecting photons from a second optical pulse as a function of time after detecting the first pulse. Although optical splitters and an optical delay line can be used with the mode-locked fiber laser source to perform this measurement as discussed in reference 3, an alternative approach to generating a train of optical pulse pairs, with a variable relative time delay, was pursued. An externally modulated CW laser was used in which pulses with variable spacing in time were generated by controlling the electrical pattern sent from a pattern generator to a pair of lithium niobate electro-optical modulators. The optical and electrical components in this setup are described in more detail in reference 6. The generated train of optical pulses was similar to that used in reference 3 to measure the recovery time of an SNSPD with the exceptions that the repetition rate was 50 MHz, rather than 10 MHz, and the duration of each optical pulse was ~ 100 ps, rather than < 1 ps. The optical intensity was adjusted such that each detector element had a $\sim$13% probability of detecting an optical pulse. In this way, the probability of detecting the second optical pulse was not substantially lower than the probability of detecting the first, regardless of the time between the optical pulses, because the detector element does not fire on the first optical pulse and is thus fully recovered $\sim$87% of the time. The electrical output from each detector element was sent to the oscilloscope and the traces from both element's outputs were saved simultaneously. These traces were post-processed using Matlab in order to determine the marginal and joint probabilities of four events during each optical pulse pair: XY where $\mathrm{X} = (\mathrm{A}, \mathrm{B})$ identifies the detector element and $\mathrm{Y} = (1, 2)$ identifies the first or second optical pulse in a pair. Thus, for a given optical pulse pair, event A1 would denote detector A firing on the first optical pulse.

Using the event probabilities calculated from the recorded oscilloscope traces, we may calculate the detection efficiency as a function of time following a detection event. We first calculate the probability of each detector element independently detecting a photon from the second optical pulse conditioned on measuring a photon from the first optical pulse. Normalizing this probability relative to the probability of detecting the second pulse when the detector is fully recovered, the probability for each detector X is: $\mathrm{P(X2|X1)/P(X2|} \sim \mathrm{X1)}$. The normalized detection efficiency is calculated by averaging this probability over $\sim$210,000 optical pulse pairs for each value of pulse separation and is shown as a function of the relative time between optical pulses for each of the two detector elements in Fig. 5 (red open squares and red x's). It is clearly seen that the probability of detecting both optical pulses with a single detector element becomes negligibly small when the optical pulses are closely spaced in time. However, the two-element detector does not have a negligible probability of detecting photons from two pulses closely spaced in time. The normalized probability of a photon from both optical pulses being detected by any combination of the two detector elements is given by $\mathrm{P(A2{+}B2|A1{+}B1)/P(A2{+}B2|} \sim \mathrm{(A1{+}B1))}$. The normalized detection efficiencies calculated from this probability for the two-element detector are also shown in Fig. 5 (black filled squares) and the detection efficiency is $\sim$ 50% when the two optical pulses are closely spaced in time. This 50% normalized detection efficiency occurs only in the low-flux limit, when it

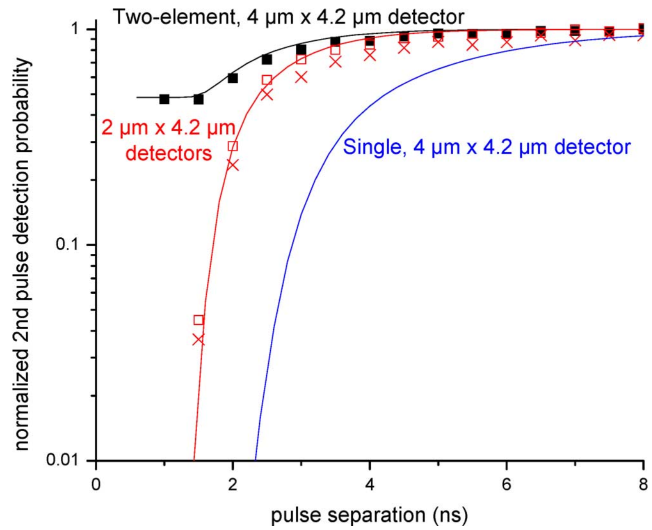

Fig. 5. Normalized probability of detecting a photon from a second optical pulse conditioned on the detection of at least one photon from the first optical pulse as a function of the optical pulse separtion. Data marked with red open squares and x's are for the two individual elements while the data marked with black closed squares is for the 2-element SNSPD. The measured inductance and detection efficiency versus bias current of the nanowires was used (see [3]) to calculate the expected recovery time for the two-element detector (black line), the single detector elements (red line), and a single detector with the same active area as the two-element detector (blue line).

is unlikely that both detector elements will fire on the first optical pulse. If only a single detector fires on the first pulse, the probability of detecting a photon from the second optical pulse is only cut by the probability the second photon is incident on the same, now inactive, element.

The recovery of the detection efficiency following a detection event was also calculated using the measured inductance and detection efficiency versus current, as described in [3]. The detection efficiency recovery for the two-element detector (black line in Fig. 5) is calculated assuming the second detector remains active 87% of the time, and must recover from simultaneously detecting a photon the remaining 13% of the time. The recovery of each element independently is also calculated and shown in Fig. 5 (red curve). Finally, the detection efficiency recovery of a device with the same active area as the two-element device is calculated by assuming its inductance is the sum of the two individual elements' inductances (blue curve in Fig. 5), because kinetic inductance dominates and is proportional to length [3]. These curves in Fig 5 clearly show that the counting rate of the two-element SNSPD is increased relative to a single SNSPD with the same active area both by the fact each element can count independently and due to the fact the kinetic inductance of each element is only half that of the entire nanowire.

IV. Conclusion

In summary, an approach for fabricating multiple superconducting nanowire single photon detector elements with a single active area has been proposed. A two-element SNSPD was fabricated and tested, and no measurable crosstalk or interactions were found between operating elements. With appropriately sized elements and suitable input optics, a MESNSPD can provide spatial and spectral information just like other arrays of photon counting detectors, but without the losses associated with coupling to independent elements. Furthermore, the MESNSPD provides the unique benefit of allowing individual elements to be smaller than a diffraction-limited optical spot when the multiple elements are intended for providing photon number resolution or higher speed. The MESNSPD is thus ideally suited to applications that can benefit from high counting rates, precise timing resolution, photon-number resolution and low optical coupling loss such as high-sensitivity classical optical communications [6] and quantum optics [9], particularly Hanbury-Brown Twiss measurements [4], [5].

Acknowledgment

The authors acknowledge D. O. Caplan, M. L. Stevens, and J. J. Carney (MIT Lincoln Laboratory) for technical assistance and Prof. H. I. Smith (MIT) for use of his equipment and facilities. This work made use of MIT's shared scanning-electron-beam-lithography facility in the Research Laboratory of Electronics.

References

[1] G. N. Gol'tsman, O. Okunev, G. Chulkova, A. Lipatov, A. Semenov, K. Smirnov, B. Voronov, A. Dzardanov, C. Williams, and R. Sobolewski, "Picosecond superconducting single-photon optical detector," *Appl. Phys. Lett.*, vol. 79, pp. 705–707, 2001.

[2] K. M. Rosfjord, J. K. W. Yang, E. A. Dauler, A. J. Kerman, V. Anant, B. Voronov, G. N. Gol'tsman, and K. K. Berggren, "Nanowire single-photon detector with an integrated optical cavity and anti-reflection coating," *Opt. Express*, vol. 14, pp. 527–534, 2006.

[3] A. J. Kerman, E. A. Dauler, W. E. Keicher, J. K. W. Yang, K. K. Berggren, G. Gol'tsman, and B. Voronov, "Kinetic-inductance-limited reset time of superconducting nanowire photon counters," *Appl. Phys. Lett.*, vol. 88, pp. 111116-1–111116-3, 2006.

[4] R. Hanbury-Brown and R. Q. Twiss, "A test of a new type of stellar interferometer on Sirius," *Nature*, vol. 178, pp. 1046–1048, 1956.

[5] R. H. Hadfield, M. J. Stevens, S. S. Gruber, A. J. Miller, R. E. Schwall, R. P. Merin, and S. W. Nam, "Single photon source characterization with a superconducting single photon detector," *Opt. Express.*, vol. 13, pp. 10846–10853, 2005.

[6] B. S. Robinson, A. J. Kerman, E. A. Dauler, R. J. Barron, D. O. Caplan, M. L. Stevens, J. J. Carney, S. A. Hamilton, J. K. W. Yang, and K. K. Berggren, "781-Mbit/s photon-counting optical communications using a superconducting nanowire detector," *Opt. Lett.*, vol. 31, pp. 444–446, 2006.

[7] P. Schwille, "Fluorescence correlation spectroscopy and its potential for intracellular applications," *Cell Biochem. and BioPhys.*, vol. 34, pp. 383–408, 2001.

[8] A. M. Wallace, G. S. Buller, and A. C. Walker, "3D imaging and ranging by time-correlated single photon counting," *Computing & Control Eng. Jour.*, vol. 12, pp. 157–168, 2001.

[9] G. Di Giuseppe, M. Atature, M. D. Shaw, A. V. Sergienko, B. E. A. Saleh, M. C. Teich, A. J. Miller, S. W. Nam, and J. Martinis, "Direct observation of photon pairs at single output port of a beam-splitter interferometer," *Phys. Rev. A*, vol. 68, pp. 063817-1–063817-4, 2003.

[10] A. D. Semenov, G. N. Gol'tsman, and A. A. Korneev, "Quantum detection by current carrying superconducting film," *Physica C*, vol. 351, pp. 349–356, 2001.

[11] A. Semenov, A. Engel, H. W. Hubers, K. Il'in, and M. Siegel, "Spectral cut-off in the efficiency of the resistive state formation caused by absorption of a single-photon in current-carrying superconducting nanostrips," *Eur. Phys. J. B*, vol. 47, pp. 495–501, 2005.

[12] V. Anant, A. J. Kerman, J. K. W. Yang, E. A. Dauler, K. M. Rosfjord, and K. K. Berggren, "Modeling the optical properties of superconducting nanowire single-photon detectors," presented at the Applied Superconductivity Conference, Seattle, WA, August 27–September 1 2006, unpublished.

[13] J. K. W. Yang, E. Dauler, A. Ferri, A. Pearlman, A. Verevkin, G. Gol'tsman, B. Voronov, R. Sobolewski, W. E. Keicher, and K. K. Berggren, "Fabrication development for nanowire GHz-counting-rate single-photon detectors," *IEEE Trans. App. Supercond.*, vol. 15, pp. 626–630, 2005.

[14] E. Knill, R. Laflamme, and G. J. Milburn, "A scheme for efficient quantum computation with linear optics," *Nature*, vol. 409, pp. 46–52, 2001.